07.2;07.3;08.2;08.3;09.1

# Investigation of the photoelectric characteristics of GaAs solar cells with different InGaAs quantum dot array positioning in the *i*-region.

© R.A Salii, M.A. Mintairov, S.A. Mintairov, M.V. Nakhimovich, M.Z. Shvarts, N.A. Kalyuzhnyy

Ioffe Institute, St. Petersburg, Russia
E-mail: r.saliy@mail.ioffe.ru

*Received June 16, 2021*
*Revised July 14, 2021*
*Accepted July 17, 2021*

The effect of positioning of the $In_{0.8}Ga_{0.2}As$ quantum dots (QDs) array in the *i*-region of the solar cell (SC) on its photogenerated current and dark saturation currents, which determine the device operating voltage, have been investigated. It was found out that the indicated photoelectric characteristics depend on the location of the QD array relative to the electric field of the $p-n$ junction. The displacement of the QD array to the boundary of the weakly doped base leads to a decrease in the photogenerated current. But at the same time, the voltage drop effect, which is well-known for nanoheterostructural SC, is minimal.

**Keywords:** solar cells, quantum dots, dark saturation current

DOI: 10.21883/TPL.2022.14.53576.18922

At present, the most efficient semiconductor solar cells (SC) are cascade devices based on the $A_3B_5$ compounds [1]. The main cause of restriction of their efficiency is current mismatch generated by the subcells of the cascade structure [2,3]. Retention of the advantage of pseudomorphous growth of the „classical" cascade GaInP/GaAs/Ge SC, jointly with overcoming the problem of the photogenerated current mismatch, is possible by using in the middle GaAs $p-n$-junction quantum-size nanoheterostructures: quantum wells, quantum dots (QD), and also hybrid objects [4–6]. However, the QDs embedment into the SC structure gives rise to the commonly known problem, namely, the drop of the device open-circuit voltage ($V_{oc}$) [7–9]. A number of studies [10,11] showed that the change in the QD array location in the SC structure can significantly affect spectral and photoelectric characteristics of the devices.

This paper demonstrates that variations in the QD positioning cause variations in the current flow mechanisms through SC, namely, changes in the dark saturation currents (DSC) that are fundamental parameters of the $p-n$-junction. For the case of marginal positions of the QD array within the *i*-region, variations in both the recombination and diffusion DSC, as well as in the current photogenerated in QD, were shown experimentally.

In addition, such studies were for the first time performed for the $In_{0.8}Ga_{0.2}As$ QDs, for which was achieved a better relaxation of stresses induced by the array in the GaAs matrix than that for „classical" InAs QD, which allows increasing the absorption medium volume without loss in the SC quantum efficiency [12].

Using the metal-organic vapor-phase epitaxy technique, four structures were grown: a reference GaAs SC without QDs (Refer), and three SC with different QD arrangement in the *i*-region. The technology of the $In_{0.8}Ga_{0.2}As$ QDs formation and description of their properties are given in [12]. In the Center-QD sample, QDs were located in the center of the *i*-region. In the Base-QD and Emitter-QD samples, QDs were displaced towards the *i*-region−base and *i*-region−emitter interfaces, respectively. All SCs, except for the reference one, contained an array of $In_{0.8}Ga_{0.2}As$ QDs consisting of five rows separated with intermediate GaAs layers 35 nm thick. On the one hand, the number of rows of deposited QDs was chosen quite small in order to make more pronounced the character of their arrangement with respect to the *i*-region electric field. On the other hand, the QD array was due to have a remarkable absorption capacity. Except for the *i*-region design, all the experimental structures were identical and contained back potential barrier *n*-$Al_{0.3}Ga_{0.7}As$, base *n*-GaAs, *i*-region $1\mu$ thick, emitter *p*-GaAs, window *p*-$Al_{0.8}Ga_{0.2}As$ and contact layer $p^+$-GaAs.

To investigate the DSC dependence on the $In_{0.8}Ga_{0.2}As$ QD array location in the *i*-region of the GaAs SC, the dependences of $V_{oc}$ on photogenerated current ($J_g$) were measured. They were obtained from a set of *J-V* characteristics at different concentration of solar radiation. The $V_{oc}$ values were related to the voltage at the zero current in the external circuit, while the photogenerated current was assumed to be equal to the short-circuit current. Since dependence $V_{oc}-J_g$ coincides with the resistance-free dark J-V characteristic [13], it is possible to use it to determine DSC values.

The $J_g$ value was calculated for the case of ground-surface solar radiation (AM1.5D, 1000 W/m$^2$) based on the data on spectral dependence of the SC external quantum yield (EQY) [14]. In the EQY measurements, facilities and technique described in paper [15] were used. The method of synchronous detection enabled sufficiently accurate fixation of the weak output signal in the QD absorption region and also sufficiently good noise suppression.

**Table 1.** Currents photogenerated by the obtained SCs with different locations of $In_{0.8}Ga_{0.2}As$ QDs in the *i*-region for two solar spectra AM0 and AM1.5.

| Sample | $J_g$, mA/cm$^2$ (AM0) | | $J_g$, mA/cm$^2$ (AM1.5) | |
|---|---|---|---|---|
| | Total (300–1100 nm) | QD (880–1100 nm) | Total (300–1100 nm) | QD (880–1100 nm) |
| Refer | 34.19 | – | 28.20 | – |
| Base-QD | 34.35 | 0.25 | 28.31 | 0.21 |
| Center-QD | 34.28 | 0.30 | 28.25 | 0.24 |
| Emitter-QD | 34.17 | 0.29 | 28.13 | 0.23 |

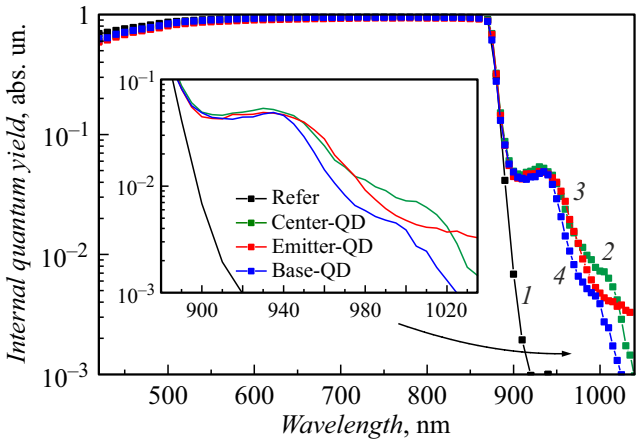


**Figure 1.** Spectra of the internal quantum yield from the obtained samples. The insert illustrates the region beyond the GaAs absorption edge.

Fig. 1 presents spectral characteristics of the internal quantum yield (IQY) obtained taking into account the spectral dependence of the reflection coefficient of the studied SCs. All the SCs exhibit the common high level of IQY in the GaAs absorption region despite different QD arrangement in the *i*-region. In the wavelength range beyond the GaAs absorption edge, broadening of the photosensitivity spectrum takes place due to absorption of subband-gap photons by the QD array (see the Fig. 1 insert). This range may be conditionally divided into two spectral regions: the contribution of the wetting layer (880–940 nm) and contribution of 3D islands (more than 940 nm). The wetting layer peak was identified based on its model presenting it as a stressed quantum well to which the electron state theory [16] was applied taking into account experimental data on its thickness and composition [17]. Since the wetting layer contribution was identified unambiguously, it is possible to state that long-wave peaks relate to the radiation absorption in QDs.

The obtained IQY spectra were used to calculate the contribution to $J_g$ from the device matrix and QD array (table 1). The comparison of $J_g$ values shows that the QD array location at the *i*-region–emitter interface, as well as in the *i*-region center, provides a greater contribution to $J_g$ in the QD absorption region (880–1100 nm). Earlier it was shown that the main contribution to the photosensitivity beyond the GaAs absorption edge comes from the wetting layer [6]. However, one can see that the Emitter-QD sample photoresponse in the long-wave region is somewhat higher.

To demonstrate the QD array location with respect to the *p*–*n*-junction electric field in different samples, band diagrams of the obtained SC structures with QDs were calculated by means AFORS-HET [18]. The code input data were the SC structure parameters (thickness, impurity concentration, electron affinity energy, band gap width, electron mass, electron velocity, band state densities, etc.), while the QD rows were input as material $In_{0.8}Ga_{0.2}As$ with the preset thickness. It was assumed that the presence of QDs does not principally change the band diagram shape. Fig. 2 presents the SC band diagrams with QDs near the conductive band. The modeled diagrams are mutually superimposed so that the conductivity band energy ($E_c$) of the QD row most distant from the emitter in the Emitter-QD sample coincides with $E_c$ of the QD row closest to the base in the Center-QD and Base-QD samples. In Fig. 2, this energy is 0.011 eV. Relative to this energy, the vacuum levels for the Emitter-QD, Center-QD and Base-QD samples are 4.55, 5.05 and 5.48 eV, respectively.

Since the minority carrier concentration in the emitter is two orders of magnitude higher than that in the base,

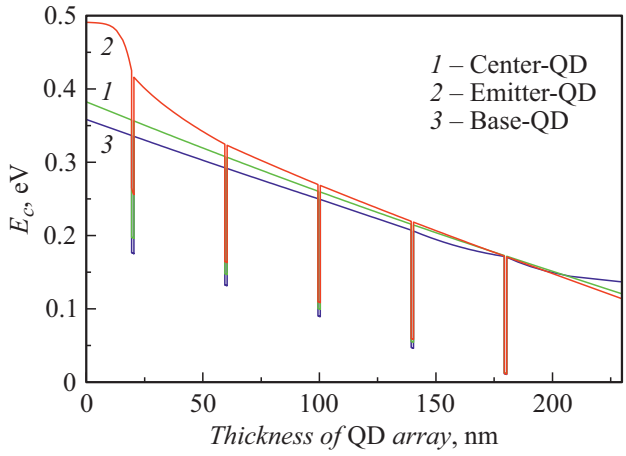


**Figure 2.** Superimposed SC band diagrams with QDs near the bottom of the QD array conduction band.

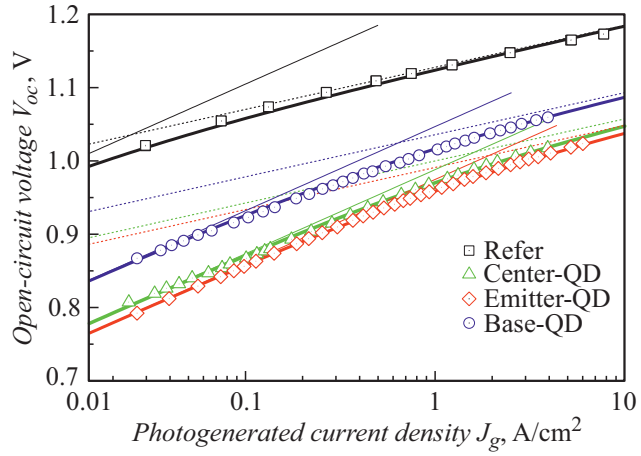


**Figure 3.** Open-circuit voltage versus the photogenerated current of studied SC (symbols) and their approximation with the two-exponential model (lines). Thin solid lines correspond to $A = 1$, thin dotted lines are for the case of $A = 2$, bold lines are their sums.

the effect of the $p-n$-junction electric field in this region is stronger than at the $i$-region–base interface. Hence, in the Emitter-QD and Center-QD samples it becomes more probable that all the charge carriers generated by subband photons will be emitted into the matrix or tunnel through the regions of the GaAs intermediate layers and then will be separated by the field and contribute to the photo current. It is also seen that (line *2* in Fig. 2) the top row of the QD array in the Emitter-QD sample is located in the strongest electric field, therefore the charge carrier emission from the QD deep levels and their separation are more probable, which explains the increase in the long-wave sensitivity of this SC.

In the Base-QD sample, the QD array is partly removed from the field (line *3* in Fig. 2), and electron-hole pairs generated in QD are likely to recombine prior to separation. Evidently, this leads to a reduction of the subband photons contribution to the total photogenerated current with respect to other SCs.

The SC-generated voltage is related with the fundamental mechanisms of the current flow in the $p-n$-junction, namely, with DSC, according to the standard two-exponential model [19]:

$$J_g = J_{0D}\exp\left(\frac{qV}{A_1kT}\right) + J_{0R}\exp\left(\frac{qV}{A_2kT}\right), \qquad (1)$$

where $J_{0D}$ and $J_{0R}$ are the diffusion and recombination DSC, respectively, $A_1$ and $A_2$ are the non-ideality factors of the $p-n$-junction (1 and 2, respectively).

Evidently, the recombination DSC ($J_{0R}$) defined by the deep-level recombination whose rate has a maximum in the space charge region will directly depend on the QD location in the $p-n$-junction field. The effect of the QD location on the diffusion DSC ($J_{0D}$) defined by the band–band recombination is less evident. However, as Fig. 2 shows, the QD array is an extended region that cannot be positioned strictly in the recombination maximum or at the interface between the regions. Therefore, it differently affects the „effective“ band gap width of the matrix, and can also affect the $J_{0D}$ value.

In order to experimentally study the influence of the QD array location on DSC and, hence, on the SC voltage, dependences of $V_{oc}$ on $J_g$ were measured (Fig. 3). The obtained curves were approximated with the two-exponential model (equation (1)) whose applicability to SCs with quantum-size objects was discussed in paper [20]. The results are listed in table 2.

Both values $J_{0D}$ and $J_{0R}$ obtained by approximating experimental dependences $V_{oc}-J_g$ exhibit the increase by two and one order of magnitude, respectively, when the QD array is introduced into the center of the GaAs SC $i$-region. The $J_{0D}$ increase leads to a conclusion that in this case the „effective“ band gap width of the $p-n$-junction decreases in the GaAs SC. Thus, the $V_{oc}$ decrease for SCs with QDs is observed in the total $J_g$ range but not only in the region where the recombination component dominates. Notice also that $J_{0D}$ changes by more than half of an order of magnitude during the QD emitter-to-base motion in the $i$-region.

Since the recombination rate has a maximum in the space charge region, $J_{0R}$ will be defined by recombination through QDs when the array is located closer to the emitter and $i$-region center. In the Base-QD sample, QDs happen to be in a weaker electric field, and $J_{0R}$ for such an SC is lower by almost an order of magnitude (table 2).

Thus, the relationship has been established of the QD array location in the SC $i$-region with DSC of the $p-n$-junction in the field of which QD are located, and also with the photogenerated current value. The larger the array inclusion into the $p-n$-junction field, the more intense the charge carrier emission into the matrix from the localization state (QD or wetting layer) and, hence, the more is the increase in $J_g$ generated by subband photons in the QD array. On the other hand, the array displacement from the region of the GaAs $p-n$-junction electric field towards, for instance, the boundary of the weakly doped base (Base-QD), results in the $J_g$ decrease, the effect of voltage drop being minimal in this case. Practically, this means that it is possible to find such a QD position in the $i$-region where the $V_{oc}$ drop is minimal with retention of the high quantum yield for the entire structure.

**Table 2.** Dark saturation currents calculated by approximating J-V characteristics with the two-exponential model.

| Sample | $J_{0D}$, mA/cm$^2$ | $J_{0R}$, mA/cm$^2$ |
|---|---|---|
| Refer | $4.0\cdot10^{-20}$ | $1.0\cdot10^{-10}$ |
| Base-QD | $1.0\cdot10^{-18}$ | $8.0\cdot10^{-10}$ |
| Center-QD | $4.2\cdot10^{-18}$ | $2.6\cdot10^{-9}$ |
| Emitter-QD | $6.0\cdot10^{-18}$ | $3.4\cdot10^{-9}$ |

### Conflict of interests

The authors declare that they have no conflict of interests.

## References


[1] P.K. Nayak, S. Mahesh, H.J. Snaith, D. Cahen, Nature Rev. Mater., **4**, 269 (2019). DOI: 10.1038/s41578-019-0097-0

[2] J.C. Algora, I. Rey-Stolle, *Handbook of concentrator photovoltaic technology* (John Wiley & Sons, U.K., 2016).

[3] M. Bonnet-Eymard, M. Boccard, G. Bugnon, F. Sculati-Meillaud, M. Despeisse, C. Ballif, Solar Energy Mater. Solar Cells, **117**, 120 (2013). DOI: 10.1016/j.solmat.2013.05.046

[4] S.A. Mintairov, N.A. Kalyuzhnyy, M.V. Maximov, A.M. Nadtochiy, S. Rouvimov, A.E. Zhukov, Electron. Lett., **51** (20), 1602 (2015). DOI: 10.1049/el.2015.2481

[5] N. Lopez, A. Marti, A. Luque, C. Stanley, C. Farmer, P. Diaz, J. Solar Energy Eng., **129**, 319 (2007). DOI: 10.1115/1.2735344

[6] N.A. Kalyuzhnyy, S.A. Mintairov, R.A. Salii, A.M. Nadtochiy, A.S. Payusov, P.N. Brunkov, V.N. Nevedomsky, M.Z. Shvarts, A. Martí, V.M. Andreev, A. Luque, Prog. Photovolt., **24** (9), 1261 (2016). DOI: 10.1002/pip.2789

[7] T. Tayagaki, Y. Hoshi, N. Usami, Sci. Rep., **3**, 2703 (2013). DOI: 10.1038/srep02703

[8] S.A. Blokhin, A.V. Sakharov, A.M. Nadtochy, A.S. Pauysov, M.V. Maximov, N.N. Ledentsov, A.R. Kovsh, S.S. Mikhrin, V.M. Lantratov, S.A. Mintairov, N.A. Kaluzhniy, M.Z. Shvarts, Semiconductors, **43** (4), 514 (2009). DOI: 10.1134/S1063782609040204.

[9] C.G. Bailey, D.V. Forbes, S.J. Polly, Z.S. Bittner, Y. Dai, C. Mackos, R.P. Raffaelle, S.M. Hubbard, IEEE J. Photovolt., **2** (3), 269 (2012). DOI: 10.1109/JPHOTOV.2012.2189047

[10] S.A. Blokhin, A.M. Nadtochiy, S.A. Mintairov, N.A. Kalyuzhny, V.M. Emel'yanov, V.N. Nevedomsky, M.Z. Shvarts, M.V. Maximov, V.M. Lantratov, N.N. Ledentsov, V.M. Ustinov, Tech. Phys. Lett., **38** (11), 1024 (2012). DOI: 10.1134/S1063785012110193.

[11] S. Chan, D. Kim, A.M. Sanchez, Y. Zhang, M. Tang, J. Wu, H. Liu, IET Optoelectron., **13** (5), 215 (2019). DOI: 10.1049/iet-opt.2018.5069

[12] R.A. Salii, S.A. Mintairov, A.M. Nadtochiy, V.N. Nevedomskii, M.Z. Shvarts, N.A. Kalyuzhnyy, Semiconductors, **54** (10), 1267 (2020). DOI: 10.1134/S1063782620100255.

[13] M. Wolf, H. Rauschenbach, Adv. Energy Convers., **3** (2), 455 (1963). DOI: 10.1016/0365-1789(63)90063-8

[14] K. Emery, *Handbook of photovoltaic science and engineering*, 2nd ed. (John Wiley & Sons, 2011). p. 797. DOI: 10.1002/9780470974704

[15] S.A. Levina, V.M. Emelyanov, E.D. Filimonov, M.A. Mintairov, M.Z. Shvarts, V.M. Andreev, Solar Energy Mater. Solar Cells, **213**, 110560 (2020). DOI: 10.1016/j.solmat.2020.110560

[16] M.P.C.M Krijn, Semicond. Sci. Technol., **6**, 27 (1991). DOI: 10.1088/0268-1242/6/1/005

[17] R.A. Salii, V.V. Evstropov, S.A. Mintairov, M.A. Mintairov, M.Z. Shvarts, N.A. Kalyuzhnyy, J. Phys.: Conf. Ser., **1410**, 012099 (2019). DOI: 10.1088/1742-6596/1410/1/012099

[18] R. Stangl, M. Kriegel, M. Schmidt, in *2006 IEEE 4th World Conf. on photovoltaic energy conversion* (IEEE, 2006), p. 1350. DOI: 10.1109/WCPEC.2006.279681

[19] W. Shockley, Bell. Syst. Tech. J., **28** (8), 435 (1949). DOI: 10.1002/j.1538-7305.1949.tb03645.x

[20] M.A. Mintairov, V.V. Evstropov, M.Z. Shvarts, S.A. Mintairov, R.A. Salii, N.A. Kalyuzhnyy, AIP Conf. Proc., **1748**, 050003 (2016). DOI: 10.1063/1.4954366